arXiv:0907.3039v2 [hep-ph] 31 Jul 2009

FERMILAB-CONF-09-358-E
DESY 09-085

Heavy flavours: working group summary

Ahmed Ali[1], Leonid Gladilin[2] and Diego Tonelli[3]

1- Deutsches Elektronen-Synchrotron DESY
Notkestrasse 85, D-22607 Hamburg - Germany

2- Moscow State University - Scobeltsyn Institute of Nuclear Physics
1(2), Leninskie gory, GSP-1, Moscow 119991 - Russia

3- Fermilab
P.O. Box 500, Batavia, IL 60510-5011 - USA

The talks presented in the working group "Heavy flavours" of the DIS 2009 workshop are summarised. New and recently updated results from theory, proton antiproton and heavy ion colliders, as well from HERA and e^+e^- colliders are discussed [1].

1 Introduction

Production and fragmentation of heavy quarks is one of the most dynamical fields of research in QCD precision tests. There is an active interplay between experimental analysis and theoretical developments in this area. The aim of the working group was to discuss the relevant experimental and theoretical results that became available or updated since the previous DIS workshop in 2008. They are summarised here in three sections: news from theory (section 2), news from proton and heavy ion colliders (section 3), and news from HERA and e^+e^- colliders (section 4).

2 News from theory

Theoretical activity in heavy flavours has been brisk during the last year, spurred by new experimental measurements and some outstanding challenges. Theory talks given in this session were invited on the following topics:

- Applications of the General-Mass Variable-Flavour-Number Scheme (GM-VFNS).
- Theoretical progress in structure functions (SFs), parton distribution functions (PDFs), fragmentation functions (FFs) and heavy flavour production cross sections.
- Studies of the $(J/\psi, \Upsilon)$ data on the production cross sections and polarisation.
- Spectroscopy of the b-baryons and interpretations of the states $X(3872)$, $Y(4140)$, and $Z^+(4430)$.

These topics were addressed in 13 theory talks. In this section, salient features of the presentations are summarised and briefly commented.

2.1 Applications of GM-VFNS

In heavy quark production processes with two large scales, m, the heavy quark mass, and p_T, the transverse momentum of the produced heavy quarks, one would like to absorb the logarithms $\ln(p_T/m)$ present in the perturbative framework, which are large in the region $p_T \gg m$, into the PDFs and FFs, where they are resummed using the DGLAP evolution as in the massless case. However, one would also like to retain the finite mass terms proportional to m^2/p_T^2 in the hard-scattering cross sections. The GM-VFNS enables to accomplish these goals in a two-step procedure: In the first step, massless and massive quark calculations are matched. The key point is to isolate the collinear singularities in the massive calculation $d\tilde{\sigma}(m)$, which are cancelled by subtracting the massless calculation (in the $\overline{\rm MS}$ scheme), $d\hat{\sigma}_{\overline{\rm MS}}$, but the residue $d\sigma_{\rm sub}$, defined as $d\sigma_{\rm sub} = \lim_{m\to 0} d\tilde{\sigma}(m) - d\hat{\sigma}_{\overline{\rm MS}}$, contains finite terms. The second step is to subtract $d\sigma_{\rm sub}$ from $d\tilde{\sigma}(m)$, the cross section with $m \neq 0$, in which the ultraviolet and collinear singularities due to massless partons have also been removed using the $\overline{\rm MS}$ factorisation scheme. The resulting cross section $d\hat{\sigma}(m) = d\tilde{\sigma}(m) - d\sigma_{\rm sub}$ is the desired quantity, in which finite quark mass terms are kept in the hard scattering cross section but the PDFs and FFs for the massless partons in the $\overline{\rm MS}$ scheme are used. Details can be seen in [2]. The GM-VFNS approach has been applied to a number of inclusive one-particle production cross sections in the processes $\gamma + \gamma \to D^{*\pm} + X$, $\gamma^* + p \to D^{*\pm} + X$, $p + \bar{p} \to (D^0, D^{*\pm}, D^{\pm}, D_s^{\pm}, \Lambda_c^{\pm}) + X$ and $p + \bar{p} \to (B^0, B^{\pm}) + X$. Of these, the photoproduction $\gamma^* + p \to D^{*\pm} + X$, open charm hadroproduction $p\bar{p} \to D + X$, and heavy quark electroproduction are being discussed in detail in these proceedings by Spiesberger [3], Kniehl [4], and Alekhin [5], respectively. In photoproduction, one has to treat consistently the contributions from the direct and resolved processes. At the next-to-leading order (NLO) theoretical precision, the separation into direct and resolved contributions becomes scheme-dependent, as the singular contributions to the direct photon part have to be factorised and absorbed into the parton distribution functions of the photon. Data on photo- and electro-production of D^* meson from H1 and ZEUS have been analysed in the GM-VFNS framework [3]. There is good overall agreement between data and theory, but the theoretical uncertainties are still large, dominated by the ambiguity in the choice of the renormalisation and factorisation scales. In the small-p_T region, theoretical prediction is uncertain by typically a factor 2 which then is propagated to the entire rapidity distributions, as they were measured with a relatively small lower cuts, $p_T > 1.8$ GeV for the photoproduction data from H1 and $p_T > 1.5$ GeV for low-Q^2 data from ZEUS. A NNLO calculation is required to reduce these uncertainties. A Monte Carlo programme for heavy quark production based on the NLO calculations has also been developed and is now in use in the analysis of the HERA data [6].

Transverse-momentum distributions for the charmed hadrons in $p\bar{p} \to (D^0, D^+, D^{*+}) + X$ are discussed in [4]. The essential improvement here is a better determination of the FFs using the LEP1, KEKB and CESR data in the GM-VFNS scheme, which has resulted in better agreement of the p_T-distributions of the charmed hadrons at the Tevatron. In the GM-VFNS scheme, D-meson hadroproduction receives contributions from the partonic processes with incoming c and $\bar{c}$, and hence this process is sensitive to their PDFs and possible intrinsic charm (IC)-induced enhancements. The IC contribution has been studied in a variety of different models and analysed in [7] using the CTEQ6.5 global analysis [8]. The p_T-distributions in $p\bar{p} \to D^0 + X$ at the Tevatron and in $pp \to D^0 + X$ at RHIC (with $\sqrt{s} = 200$ GeV and $\sqrt{s} = 500$ GeV) have been calculated in the GM-VFNS scheme and the

former are compared with the Tevatron data, using six different parameterisations of the IC-contribution. Unfortunately, no firm conclusions can be drawn as the present Tevatron data, which is of the 2002 vintage, is based on rather modest luminosity ($5.8\,\mathrm{pb}^{-1}$). This will change greatly if the full force of the current Tevatron integrated luminosity (circa $5\,\mathrm{fb}^{-1}$) is brought to bear on this analysis. Data at RHIC are also potentially sensitive to the input IC-contribution and will be able to discriminate among the various IC-models in the future.

The charm structure function $F_2^{c\bar{c}}(x,Q^2)$ measured in the DIS electroproduction at HERA was discussed by Alekhin [5] in the context of the two schemes FFNS (fixed flavour-number scheme) and the VFNS, using the Buza-Matiounine-Smith-van Neerven (BMSN) prescription [9]. The main conclusion from this analysis is that for the realistic HERA kinematics, the two schemes are rather similar. FFNS with partial $O(\alpha_s^3)$ corrections incorporated provides a good description of the HERA data for small/moderate Q^2 values, but it undershoots the data for high Q^2, calling for including the remaining $O(\alpha_s^3)$ pieces. Finally, an intermediate mass scheme was discussed by Nadolsky [10] and a global PDF analysis was carried out in this scheme with the conclusion that the intermediate-mass formulation improves the NLO zero-mass scheme and approximates the more fundamental General-mass scheme (GM-VFNS) in a simple way.

2.2 Progress in structure functions involving heavy quarks

State of the art QCD analysis requires the description of the heavy quark contribution to the structure functions at 3 loops to match the accuracy reached in the massless partonic case. Making use of the factorisation property of the heavy quark Wilson coefficients, denoted by $H_{(2,L),j}$, into a product of the massive operator matrix elements $A_{kj}^{S,NS}$, and the light flavour Wilson coefficients $C_{(2,L),k}^{S,NS}$, which holds in the region $Q^2 \gg m^2$, one has

$$H_{(2,L),j}^{S,NS}\left(\frac{Q^2}{\mu^2},\frac{m^2}{\mu^2}\right) = A_{kj}^{S,NS}\left(\frac{m^2}{\mu^2}\right) \otimes C_{(2,L),k}^{S,NS}\left(\frac{Q^2}{\mu^2}\right) \ . \tag{1}$$

Analytic results are known for $Q^2 \gg m^2$ at NLO for $F_2(x,Q^2)$ and at NNLO for $F_L(x,Q^2)$. The light flavour Wilson coefficients are also known at the NNLO, thanks to the formidable calculation by Vermaseren, Vogt and Moch [11]. At this conference, massive operator matrix elements $A_{kj}^{S,NS}(\frac{m^2}{\mu^2})$, contributing to $F_2(x,Q^2)$ were reported in the region $Q^2/m^2 \geq 10$ to 3-loop accuracy for the fixed moments of the Mellin variable N [12]. In a computational *Tour de force*, the following fixed moments of the massive operator matrix elements were accomplished [13]:

$$\begin{aligned} A_{Qq}^{(3),\mathrm{PS}}: &\quad (2,4,...,12); \quad A_{qq,Q}^{(3),\mathrm{PS}}, A_{gq,Q}^{(3)}: (2,4,...,14)\ ; \\ A_{qq,Q}^{(3),\mathrm{NS}\pm}: &\quad (2,3,...,14); \quad A_{Q(q)g}^{(3)}, A_{gg,Q}^{(3)}: (2,4,...,10)\ . \end{aligned} \tag{2}$$

The superscript PS(NS) stands for the pure singlet (non-singlet) case, and the quarkonic operator matrix element is represented as $A_{qq}^{S} = A_{qq}^{NS} + A_{qq}^{PS}$. In the case of the flavour non-singlet contributions, also the odd moments are calculated. This provides an independent check on the 3-loop anomalous dimensions $\gamma_{qg}^{(2)}$, $\gamma_{qq}^{(2),PS}$ and on the respective colour projections of $\gamma_{qq}^{(2),NS\pm}$, $\gamma_{gg}^{(2)}$ and $\gamma_{gq}^{(2)}$. Phenomenological parameterisations are to follow soon.

Heavy flavour effects in the virtual photon structure functions in the NLO accuracy were reported at this meeting by Uematsu [14]. Concentrating on $F_2^\gamma(x,Q^2,P^2)$, where Q^2 is the photon virtuality and P^2 the target (photon) mass, one has the factorisation result as a convolution in the virtual photon distribution function $\vec{q}^\gamma$ and the coefficient function $\vec{C}$

$$F_2^\gamma(x,Q^2,P^2) = \vec{q}^\gamma(y,Q^2,P^2,m^2) \otimes \vec{C}\left(\frac{x}{y},\frac{\bar{m}^2}{Q^2},\bar{g}(Q^2)\right) \ , \tag{3}$$

where the heavy quark mass dependence enters in both the terms. Taking the moments of $\vec{q}^\gamma$, one can write the resulting expression as a product of two terms

$$\int_0^1 dx x^{n-1}\vec{q}^\gamma(x,Q^2,P^2,m^2) = \vec{A}_n\left(1,\frac{\bar{m}^2(P^2)}{P^2},\bar{g}(P^2)\right) T\exp\left[\int_{\bar{g}(Q^2)}^{\bar{g}(P^2)} dg\frac{\gamma_n(g,\alpha)}{\beta(g)}\right], \tag{4}$$

where the matrix element

$$\langle\gamma(P^2)|\vec{O}_n(\mu^2)|\gamma(P^2)\rangle = \vec{A}_n\left(\frac{P^2}{\mu^2},\frac{\bar{m}^2(\mu^2)}{\mu^2},\bar{g}(\mu^2)\right) \tag{5}$$

is perturbatively calculable. Thus, as opposed to the nucleon structure functions discussed above, the photon structure function is completely calculable perturbatively, as first emphasised by Witten [15]. This framework has been applied in the massive quark limit $\Lambda^2_{\rm QCD} \ll P^2 \ll m^2 \ll Q^2$ to the PLUTO data with $Q^2 = 5$ GeV^2 and $P^2 = 0.35$ GeV^2, with the conclusion that the data is in better agreement with the case of 3 massless NLO QCD + c massive compared to the 4 massless NLO QCD case [16]. A comparison of the massive b quark + 4 massless quarks case with the L3 data for $Q^2 = 120$ GeV^2 and $P^2 = 3.7\,$GeV^2 is not as conclusive due to the smaller $(-1/3)$ electric charge of the b-quark as well as the imprecise nature of the L3 data.

2.3 Progress in the $t\bar{t}$ production cross section at the Tevatron and the LHC

There has been steady progress in calculating the $t\bar{t}$ production cross section at the Tevatron and the LHC. This was reported at this conference by Langenfeld [17], and since then in a recently published paper [18], in which the cross section at the Tevatron is used to determine the running top quark mass. The relevant formulae for the process $\sigma(pp(\bar{p}) \to t\bar{t}+X)$ are:

$$\sigma(pp(\bar{p}) \to t\bar{t}+X) = \frac{\alpha_s^2}{m_t^2}\sum_{i,j=q,\bar{q},g}\int_{4m_t^2}^S ds L_{ij}(s,S,\mu_f^2) f_{ij}(\rho,M,R) \ , \tag{6}$$

$$L_{ij}(s,S,\mu_f^2) = \frac{1}{S}\int_s^S \frac{d\hat{s}}{\hat{s}}\phi_{i/p}\left(\frac{\hat{s}}{S},\mu_f^2\right)\phi_{j/p(\bar{p})}\left(\frac{s}{\hat{s}},\mu_f^2\right) \ , \tag{7}$$

Here, S is the centre-of-mass energy squared (of the pp or $p\bar{p}$ colliding beams), s is the partonic centre-of-mass energy squared, m_t is the top quark (pole) mass, and L_{ij} is the parton luminosity function with the PDFs ϕ_i/p, evaluated at the factorisation scale μ_f. The functions $f_{ij}(\rho,M,R)$ are the hard partonic cross section and depend on the dimensionless variables $\rho = 4m_t^2/s$, $R = \mu_r^2/\mu_f^2$ and $M = \mu_f^2/m_t^2$, where μ_r is the renormalisation scale. They have been solved in perturbation theory up to two loops. For $M = R = 1$, i.e.,

$m_t = \mu_r = \mu_f$, one has $f_{ij}(\rho, 1, 1) = f_{ij}^{(0)}(\rho) + 4\pi\alpha_s f_{ij}^{(1)}(\rho) + (4\pi\alpha_s)^2 f_{ij}^{(2)}$. The dependence of $f_{ij}(\rho, M, R)$ on the scales μ_f and μ_r can be made explicit and the expressions can be seen in [18]. Up to one loop, the results are known since long, and at the two-loop level, the corrections include the Sudakov logarithms $\ln^k \beta$, where β is the t-quark velocity, $\beta = \sqrt{1-\rho}$, and terms with $k = 1, ..., 4$ are included in $f_{q\bar{q}}^{(2)}$ and $f_{gg}^{(2)}$ (the leading term $\sim \ln^3 \beta$ in $f_{qg}^{(2)}$), as well as the Coulomb contributions $\sim 1/\beta^2, 1/\beta$. The subleading correction in the function $f_{ij}^{(2)}$ has yet to be calculated. Estimating it as $O(30\%)$ in the NNLO contribution implies an uncertainty of $\Delta\sigma(pp \to t\bar{t} + X) = \mathcal{O}(15)$ pb at the LHC and $\Delta\sigma(p\bar{p} \to t\bar{t} + X) = \mathcal{O}(0.2)$ pb at the Tevatron. The rest of the uncertainties come from the PDFs, the scales μ_f and μ_r, α_s and m_t. For the pole mass $m_t = 173$ GeV, the $t\bar{t}$ cross sections at the LHC ($\sqrt{S} = 14$ TeV) and the Tevatron ($\sqrt{S} = 1.96$ TeV) are estimated (for the MSTW2008 PDFs [19]) as follows [18]:

$$\sigma(pp \to t\bar{t} + X)_{\rm LHC} = (887^{+9}_{-33}(\text{scale}) \pm 15(\text{PDF}))\ \text{pb}\ , \tag{8}$$

$$\sigma(p\bar{p} \to t\bar{t} + X)_{\rm Tevatron} = (7.04^{+0.24}_{-0.36}(\text{scale}) \pm 0.14(\text{PDF}))\ \text{pb}\ . \tag{9}$$

For the CTEQ6.6 set of PDFs [20], the central values of the cross section become 874 pb and 7.34 pb, for the LHC and the Tevatron, respectively, with almost the same scale uncertainties as for the MSTW2008 PDFs, but the PDF-related errors for this set are significantly larger, ± 28 pb in $\sigma_{\rm LHC}$ and ± 0.41 pb in $\sigma_{\rm Tevatron}$, respectively. Finally, using the well-known relation between the pole mass m_t and the $\overline{\rm MS}$ mass $\bar{m}_t(\mu_r = \bar{m}_t)$, and making the m_t-dependence in the total cross section manifest, a value $\bar{m}_t(\bar{m}_t) = 160.0^{+3.3}_{-3.2}$ GeV for the $\overline{\rm MS}$ top quark mass is obtained from the Tevatron production cross section.

2.4 Theoretical status of J/ψ production at HERA

The cross section $\sigma(\gamma p \to J/\psi + X)$ in the colour-singlet (CS) model at the NLO accuracy was calculated some time ago by Krämer [21] and has been reconfirmed recently in [22], in which polarisation observables in photoproduction were also calculated at the NLO accuracy. These calculations have been compared with the published [23] and preliminary ZEUS data [24] and the results are summarised at this conference by Artoisenet [25]. The hadronic matrix element $\langle \mathcal{O}_{J/\psi}(^3S_1)[1] \rangle$ was fixed from the analysis of the J/ψ-hadroproduction data and the CTEQ6M PDF set [26] was used. The three main phenomenological parameters m_c, the charm quark mass, and μ_r, μ_f, the renormalisation and factorisation scales, were varied in the range 1.4 GeV $< m_c <$ 1.6 GeV, $\mu_0 = 4m_c$, $0.5\mu_0 < \mu_r, \mu_f < 2\mu_0$, and $0.5 < \mu_r/\mu_f < 2$. It was found that the CS yield at NLO accuracy underestimates the ZEUS data in both the p_T and z-distributions, where $z = p_\psi.p_p/p_\gamma.p_p$ – a conclusion which is at variance with the observations made earlier [23]. The polarisation of J/ψ is studied by analysing the angular distributions of the leptons originating from the decay $J/\psi \to \ell^+\ell^-$. In terms of the polar and azimuthal angles θ and ϕ in the J/ψ rest frame, one has

$$\frac{d\sigma}{d\Omega dy} \propto 1 + \lambda(y)\cos^2\theta + \mu(y)\sin 2\theta\cos\phi + \frac{\nu(y)}{2}\sin^2\theta\cos 2\phi\ , \tag{10}$$

where y stands for either p_T or z. If the polar axis coincides with the spin quantisation axis, the quantities $\lambda(y)$, $\mu(y)$ and $\nu(y)$ can be related to the spin density matrix elements. The $O(\alpha_s)$ corrections in the CS model have a strong impact on the polarisation parameters ν

and λ, which were analysed as functions of p_T and z. In particular, the λ-distribution in NLO decreases rapidly with increasing p_T and has a large negative value above $p_T = 4$ GeV, in contrast to the LO prediction, which is in reasonably good agreement with the data. The measurements of the parameter ν are, on the other hand, in better agreement with the NLO predictions (compared to the LO CS model prediction), though the model uncertainties are too large for low z values to draw a quantitative conclusion.

On a related issue, Faccioli [27] summarised the experimental situation of J/ψ polarisation from the fixed target (E866, HERA-B) to the collider energies (CDF), observing that the magnitude and the "sign" of the measured J/ψ polarisation crucially depends on the reference frame [28]. In particular, he showed that the seemingly contradictory data on the parameter λ from the experiments E866, HERA-B and CDF overlap as a function of the J/ψ cms total momentum and the data can be consistently described, assuming that the most suitable axis for the measurement is along the direction of the relative motion of the colliding partons. In this (Collins-Soper) frame, polarisation changes from the longitudinal at small momentum to transverse at high momentum. This resolves the apparent J/ψ polarisation puzzle among the experiments. However, the puzzle involving the theory (based on NRQCD) vs. experiment still persists. In conclusion, a quantitative understanding of the J/ψ-photoproduction data at HERA is still lacking, calling for improved calculations within the NRQCD (such as invoking colour-octet transitions and $O(\alpha_s^2)$ corrections to the CS model) or perhaps the J/ψ data are inviting a better theoretical framework. Soft Collinear Effective Theory is a case in point. A theoretical analysis of the production cross section and the spin alignment parameter $\alpha(\Upsilon)$ in $p\bar{p} \to \Upsilon + X$ data from the D0 collaboration at the Tevatron was presented by Zotov [29], with very similar conclusion, namely that the existing QCD framework is not in agreement with the data, in particular the distribution of $\alpha(\Upsilon)$ as a function of p_T is not understood. This will come under sharp scrutiny at the Tevatron and certainly at the LHC.

2.5 New developments in the spectroscopy of charm and beauty hadrons

The saga of the successful predictions of the constituent quark model (CQM) continues! Salient features of the b-baryon spectroscopy in this model were discussed and contrasted with the existing data by Karliner [30], with the conclusion that CQM (with colour hyperfine interaction) gives a highly accurate predictions for the heavy baryon masses. Four examples from the b-baryon spectroscopy illustrate this: The measured mass difference by the CDF collaboration $m(\Sigma_b) - m(\Lambda_b) = 192$ MeV was predicted to be 194 MeV; the hyperfine splitting $m(\Sigma_b^*) - m(\Sigma_b) = 21$ MeV [CDF] is in agreement with the predicted value of 22 MeV. Likewise, the predictions for the masses, $m(\Xi_b) = 5795 \pm 5$ MeV vs. $5793 \pm 2.4 \pm 1.7$ MeV (expt.), and $m(\Omega_b) = 6052.9 \pm 3.7$ MeV, vs. $m(\Omega_b) = 6054.4 \pm 6.8$ (stat) ± 0.9 (syst.) MeV [CDF], are in excellent agreement with data. It should, however, be noted that the measurement of the Ω_b mass by CDF [31] differs from the first reported measurement of the Ω_b^- mass by D0, $m(\Omega_b^-) = 6165 \pm 10(\text{stat}) \pm 13(\text{syst})$ MeV [32]. On the theoretical side, the aspect that the constituent quark masses in this model, in particular the mass difference $m_b - m_c$ used as input, depend on the spectator quarks, deserves further study. Thus, the relation of the CQM with QCD, in which quark masses are universal, is far from obvious.

The observation of the narrow state $X(3872)$ by BELLE, in the decay mode $B^\pm \to K^\pm \pi^+ \pi^- J/\psi$, with the $\pi^+\pi^- J/\psi$-mass spectrum peaking at 3872 MeV, dominated by the state $X(3872) \to J/\psi\rho$, as well as the radiative decay mode $X(3872) \to J/\psi\gamma$, measured by

BABAR, has established $X(3872)$ as an exotic $J^{\rm PC} = 1^{++}$ state. CDF and D0 confirmed the $X(3872)$ in $p\bar{p}$ collisions (produced predominantly in prompt processes rather than in B decays). In addition, the decay mode $X(3872) \to J/\psi\omega$, which seems to have a similar branching ratio as the mode $X(3872) \to J/\psi\rho$, implies large isospin violation, not typical of the usual strong interactions. The two leading hypotheses are that $X(3872)$ is a loosely bound "hadronic molecule" of the $D^0\bar{D}^{0*}$, since the mass of $X(3872)$ is so close to the $D^0\bar{D}^{0*}$ threshold [33], or that it is a point-like hadron, a tightly bound state of a diquark and an antidiquark, a tetraquark [34]. The drawback of the tetraquark picture is that it predicts a very rich spectroscopy. However, one has little understanding why a large number of these states have not been found. One of these predictions, namely the existence of related charged particles decaying into charmonium and pions, is still being debated. The molecular picture seems to be at odds with the large prompt production in hadronic collisions. At this conference, Polosa [35] presented a calculation for the production cross section of $X(3872)$ at the Tevatron, assuming that $X(3872)$ is a loosely bound $D^0\bar{D}^{0*}$ molecule. Since then, this work has been published [36] and the main points are summarised here. Using the CDF data on prompt $X(3872)$ production in the $J/\psi\pi^+\pi^-$ mode and the yield of $\psi(2S) \to J/\psi\pi^+\pi^-$, as well as the fraction of the prompt $\psi(2S)$ candidates, and assuming that the $X(3872)$ and $\psi(2S)$ have the same rapidity distribution in the range $|y| < 1$, a lower bound on the prompt production cross section $\sigma(p\bar{p} \to X(3872) + X)$ of 3.1 ± 0.7 nb is obtained. This is contrasted with the estimates of an upper bound on the theoretical cross section, based on the assumption that $X(3872)$ is an S-wave bound state, $X(3872) = 1/\sqrt{2}(D^0\bar{D}^{*0} + \bar{D}^0 D^{*0})$:

$$\sigma(p\bar{p} \to X(3872) + X) \propto |\int d^3\mathbf{k} \langle X|D\bar{D}^*(\mathbf{k})\rangle\langle D\bar{D}^*(\mathbf{k})|p\bar{p}\rangle|^2 \leq \int_{\mathcal{R}} d^3\mathbf{k} |\langle D\bar{D}^*(\mathbf{k})|p\bar{p}\rangle|^2 \ , \tag{11}$$

where $\mathbf{k}$ is the relative 3-momentum between the $D(\mathbf{p}_1)$ and $D^*(\mathbf{p}_2)$ mesons. $\psi(\mathbf{k}) = \langle X|D\bar{D}^*(\mathbf{k})\rangle$ is a normalised wave function for the state $X(3872)$, and $\mathcal{R}$ is the region where $\psi(\mathbf{k})$ is non-zero. The matrix element $\langle D\bar{D}^*(\mathbf{k})|p\bar{p}\rangle$ is calculated with the help of QCD ($2 \to 2$) matrix elements embedded in the fragmentation programme, Pythia and Herwig. With the binding energy $\mathcal{E}_0 \sim M_X - M_D - M_{D^*} = -0.25 \pm 0.40$ MeV, the characteristic size r_0 of the molecule is estimated as $r_0 \sim (8.6 \pm 1.1)$ fm, yielding for k a number $k \simeq \sqrt{\mu(-0.25 \pm 0.40)} \simeq 17$ MeV, where $\mu = m_D m_{D^*}/(m_D + m_{D^*})$ is the reduced mass. Applying the uncertainty principle yields a Gaussian momentum spread $\Delta p \sim 12$ MeV. Alternatively, k is of the order of the centre of mass momentum, $k \simeq 27$ MeV. With this, the integration region is restricted to a ball $\mathcal{R}$ of radius $\simeq [0, 35]$ MeV. Herwig then yields an upper limit of 0.013 nb on $\sigma(p\bar{p} \to X(3872) + X)$ and the corresponding number for Pythia is 0.036 nb. This is typically two orders of magnitude smaller than the measured cross section by CDF, disfavouring the molecular interpretation of $X(3872)$.

3 News from proton and heavy ion colliders

3.1 New results from $p\bar{p}$ and pp colliders

The Tevatron is today the only environment where all species of heavy flavours (HF) are studied. The CDF and D0 experiments pursue a rich and diverse HF program that is reaching maturity, owing to samples of $p\bar{p}$ collisions in excess of 5 fb^{-1} per experiment, expected to double by 2011. This suggests a few years of intense and fruitful competition with next generation experiments that will soon start their operations at the LHC.

With thousands of top-quark decays collected, Tevatron top physics entered the realm of precision [37]. Using 2.8 fb^{-1} CDF reported the single most precise $t\bar{t}$ production cross section measurement, $\sigma_{t\bar{t}} = 6.9 \pm 0.4(\text{stat}) \pm 0.4(\text{syst}) \pm 0.1(\text{theo})$ pb; the 8% relative uncertainty challenges the precision of most recent theory predictions, and is achieved by normalising the $t\bar{t}$ to the Z cross section thus cancelling the leading systematic uncertainty from the luminosity of the sample. D0 reports a result, combined through 14 independent channels, of $\sigma_{t\bar{t}} = 8.18^{+0.98}_{-0.87}$ pb using 0.9 fb^{-1}. While measurements of $t\bar{t}$ strong production are an important test of perturbative QCD, electroweak (single) top-quark production determines directly the magnitude of the V_{tb} quark-mixing matrix element, probes the b–quark PDF of the proton, is sensitive to fourth generation models, and is ultimately a key testing ground for Higgs searches in the WH associated production channel. Both experiments reported 5σ observation of this process using 2.3 (D0) and 3.2 (CDF) fb^{-1}. Because of the tiny signal-to-background ratio, use of advanced machine-learning techniques is required, whose performance is carefully validated in multiple control samples. The measured cross sections, $\sigma_t = 2.3^{+0.6}_{-0.5}$ pb (CDF) and $\sigma_t = 3.94 \pm 0.88$ pb (D0), yield the values $|V_{tb}| = 0.91 \pm 0.13$ (CDF) and $|V_{tb}| = 1.07 \pm 0.12$ (D0).

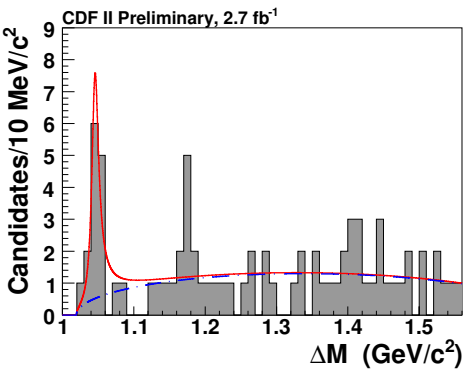

Figure 1: Difference between the $J/\psi\phi$ and the J/ψ mass as observed by CDF in 2.7 fb^{-1} of Tevatron $p\bar{p}$ data with fit projection in the background-only (dashed line) and signal +background hypothesis (full line) overlaid.

Interest in HF spectroscopy was renewed recently, after a few unexpected "exotic" states, observed at the B factories, challenged our understanding of hadrons' composition [38]. The latest addition to this picture comes from CDF, which reports evidence of a new resonant $J/\psi\phi$ state, reconstructed from the world's largest sample ($\approx$ 75 events) of $B^+ \to J/\psi\phi K^+$ decays, in 2.7 fb^{-1} of data. The excess amounts to 14 ± 5 events, for a significance in excess of 3.8σ (Fig. 1). The particle is dubbed $Y(4140)$ after its observed mass of $4143 \pm 2.9(\text{stat}) \pm 1.2$ (syst) MeV, which is above the charm-pair threshold and disfavours interpretations as a conventional charmonium state. D0 reports the first observation of the Ω_b^+ baryon (quark content ssb) in its $J/\psi(\to \mu\mu)\Omega^+[\to \Lambda(\to p\pi)K^+]$ decay with 18 ± 5 events in 1.3 fb^{-1} and a significance greater than 5σ (Fig. 2). The observed mass value, $m(\Omega_b^+) = 6165 \pm 10(\text{stat}) \pm 13$ (syst)

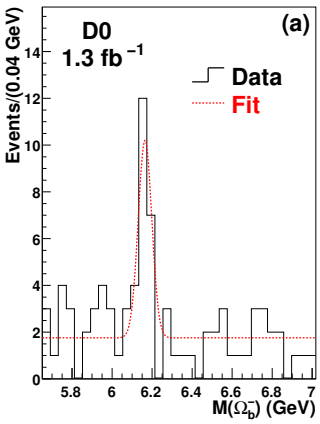

Figure 2: Mass distribution of Ω_b^+ candidates reconstructed by D0 in 1.3 fb^{-1} of Tevatron $p\bar{p}$ data with fit projection overlaid.

MeV, is higher than most theoretical predictions. Shortly after this workshop, CDF has reported observation of this baryon with mass $6054.4 \pm 6.8(\text{stat}) \pm 0.9$ (syst) [31], in good agreement with theoretical expectations [30].

Hadroproduction of HF is a crucial test of our understanding of QCD [39]. CDF presented a measurement of B_c^+ production cross section in the semileptonic $J/\psi(\to \mu^+\mu^-)\mu^+X$ final state using $B^+ \to J/\psi K^+$ as a reference. The ratio of production rates times branching ratios in the $p_T > 4\,\text{GeV}$ regime is $R = 0.295 \pm 0.063$, using $1\,\text{fb}^{-1}$. CDF also reconstructed a few hundred events in the exclusive channel $B_c^+ \to J/\psi\pi^+$ using the full $4.7\ \text{fb}^{-1}$ sample. A signal with similar yield and purity is expected from LHCb with just $1\ \text{fb}^{-1}$ of data. However, the general common strategy for initial measurements at LHC is to focus on either inclusive final states or well-known exclusive ones, like $B^+ \to J/\psi K^+$. The LHC experiments plan to provide a deeper insight into some theory/data discrepancies observed in prompt *onia* production (spectra and polarisations) at the Tevatron. Even with a small fraction of their initial data, significant samples are expected, by exploiting larger and complementary detector acceptances with respect to CDF and D0: e.g. CMS expects $\approx 75,000$ J/ψ decays in only $3\ \text{pb}^{-1}$ of data.

CDF also reported the first observation of exclusive central charmonium (photo)production [40] in hadron collisions. Clear J/ψ and $\psi(2S)$ signals over a negligible continuum background are reconstructed, in agreement with theory predictions. Observation of exclusive χ_{c0} production as well provides useful constraints on the reach in exclusive Higgs production at the LHC.

3.2 New results from heavy ion colliders

The era of "beauty" is opening at RHIC [41]. Heavy flavours are key tools to probe and understand independently of other methods the properties of the hot and dense nuclear medium through their energy loss. Both the STAR and PHENIX experiments reconstruct $\Upsilon \to e^+e^-$ signals in $\sqrt{s} = 200$ GeV pp (Fig. 3, left) and d+Au collisions, and observe binary scaling of the production. Production of quarkonia is not modified in d+Au collisions (e.g. STAR measures $R_{d\text{Au}} = 0.98 \pm 0.32(\text{stat}) \pm 0.28(\text{syst})$) but appears suppressed in Au+Au collisions, which is not fully understood. In addition, both experiments find large b–quark contribution to the single-e spectrum at $p_T > 4$ GeV, in agreement with FONLL pQCD theory [42] (Fig. 3, right). Next generation heavy ions experiments plan to improve these results and obtain a clearer picture: in just one month of running ALICE plans to collect large samples of *onia* with significances $S/\sqrt{S+B} \approx 10 - 100$. Similarly, CMS plans to efficiently reconstruct charmonia and bottomonia in Pb+Pb collisions and be able to determine the production cross section [43].

4 News from HERA and e^+e^- colliders

4.1 New results from e^+e^- colliders

An observation of an anomalous line-shape of the $e^+e^- \to$hadrons cross sections near 3.770 GeV has been reported by BES [44]. It is inconsistent with only one $\psi(3770)$ state, suggesting either a new structure in addition to the $\psi(3770)$ resonance or some physics effects distorting the pure D-wave Breit-Wigner shape of the cross sections. The observation suggests that a surprisingly large non-$D\bar{D}$ branching fraction of the $\psi(3770)$ decays mea-

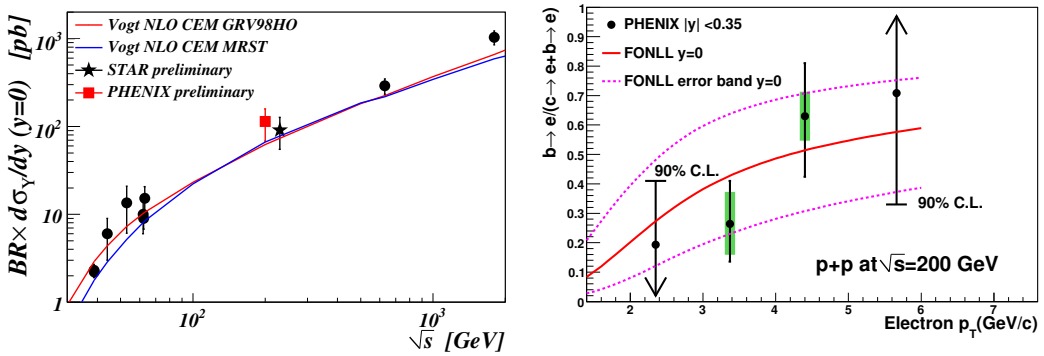

Figure 3: Left – cross section for Υ production times branching ratio as a function of centre-of-mass energy. PHENIX and STAR data points are shown as well as theory predictions. Right – bottom fraction as a function of electron p_T measured in PHENIX data (points), compared to the FONLL prediction (solid line) and its uncertainty (dashed lines).

sured previously by BES [44] may partially be due to the assumption of only one simple resonance near 3.770 GeV.

Recent measurements of the leptonic and semileptonic D^0, D^+ and D_s^+ branching fractions have been reported by CLEO [44]. Using lattice QCD calculations, the $|V_{cs}|$ and $|V_{cd}|$ elements of the CKM matrix were determined and found to be in agreement with previous measurements.

New BELLE measurement of the $X(3872) \to D^0 \bar{D}^{*0}$ decay [45] has revealed the X mass value of $3872.6^{+0.5}_{-0.4} \pm 0.4$ MeV in fair agreement with the mass measurement in the dominant $X(3872) \to J/\psi\pi\pi$ decay mode. A first evidence for the $X(3872) \to \psi(2S)\gamma$ decay reported by BABAR [45] has allowed to determine the ratio of the branching fractions

$$\mathcal{B}_{X\to\psi(2S)\gamma}/\mathcal{B}_{X\to J\psi\gamma} = 3.4 \pm 1.4\,,$$

which is above the molecule model expectation [46].

The situation with the charged state $Z^+(4430)$ remains unclear [45]. BELLE has confirmed its observation by the Dalitz plot analysis of the $Z^+(4430) \to \psi(2S)\pi^+$ decay [45]. However, BABAR has found no evidence for the charged state in the above decay and in the $J/\psi\pi^+$ final state. Meanwhile, BELLE has reported two further charged states $Z(4050/4250)^+ \to \chi_{c1}\pi^+$.

BABAR has confirmed its observation of the $\eta_b(1S)$ bottomonium ground state in the decay $Y(3S) \to \gamma\eta_b(1S)$ by a new $\eta_b(1S)$ measurement in the $Y(2S) \to \gamma\eta_b(1S)$ decay [47]. Searches for the light Higgs-like particle in the $Y(2S)$ and $Y(3S)$ radiative decays have revealed no signal.

4.2 New HERA results

New measurement of J/ψ production in proton-nucleus collisions performed by HERA-B [48] has confirmed that the dN/dp_T distribution becomes broader with increasing atomic mass number, A. The dN/dx_F distribution also tends to become broader and its centre moves towards negative x_F values with increasing A. The fraction of J/ψ mesons produced through

the χ_c decay has been measured to be $R_{\chi_c} = 18.8 \pm 1.3^{+2.4}_{-2.2}\,\%$ with a ratio of χ_{c1} and χ_{c2} contributions $R_{\chi_{c1}}/R_{\chi_{c2}} = 1.02 \pm 0.20$ [48]. The measured J/ψ decay angular distributions indicate the polar anisotropy with a preferred spin component 0 along the reference axis. The polar anisotropy increases with decreasing $p_T(J/\psi)$ [48]. The J/ψ helicity distributions measured by ZEUS in the inelastic photoproduction regime [49] have been compared to LO QCD predictions in the colour-singlet, colour-singlet plus colour-octet and k_T factorisation approaches; none of the predictions can describe all aspects of the data.

Charm fragmentation function in the transition from a charm quark to a D^{*+} meson measured by ZEUS using the variable $z = (E + p_{||})^{D^{*+}}/2E^{jet}$ [50] is compared in Fig. 4 with previous measurements from BELLE, CLEO and ALEPH. The corresponding scale of the ZEUS data is given by twice the average transverse energy of the jet, 23.6 GeV, and is between the two e^+e^- centre-of-mass energies. The ZEUS data in Fig. 4 are shifted somewhat to lower values of z compared to the CLEO and BELLE data with the ALEPH data even lower, which is consistent with the expectations from the scaling violations in QCD. The value of the free parameter in the Peterson *et al.* fragmentation function [51] extracted from the ZEUS data within the framework of the next-to-leading order (NLO) QCD, $\epsilon = 0.079 \pm 0.008^{+0.010}_{-0.005}$, exceeds the value 0.035 obtained from an NLO fit [52] to the ARGUS data.

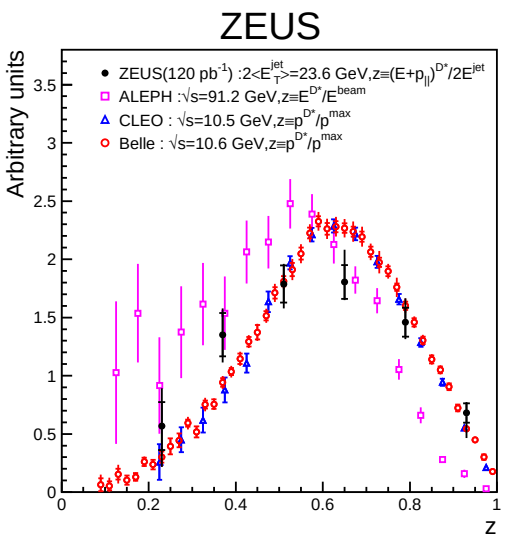

Figure 4: Charm fragmentation function in transition to D^{*+} for the ZEUS data compared to measurements of BELLE, CLEO and ALEPH.

Sizable production of the excited charm and charm-strange mesons has been observed in ep interactions by ZEUS [50]. The fractions of c quarks hadronising into D_1^0, D_2^{*0} or D_{s1}^+ mesons are consistent with those obtained in e^+e^- annihilations. The measured D_1^0 width, $\Gamma(D_1^0) = 53.2 \pm 7.2^{+3.3}_{-4.9}$ MeV, is above the world average value. This is possibly due to a larger admixture from the broad S-wave decay at ZEUS compared to the measurements with restricted phase space [50].

New measurements of beauty dijet photoproduction have been performed by H1 [53], using events with a muon in the final state, and ZEUS [54]. The production cross sections were found to be compatible with the previous HERA measurements and with NLO QCD predictions. The measured cross sections translated into a differential cross section $\frac{d\sigma}{dp_T^b}$ in the pseudorapidity range $|\eta_b| < 2$ are compared to the previous HERA measurements and the FMNR NLO QCD predictions [55] in Fig. 5.

Inclusive production of $D^{*\pm}$ mesons in deep inelastic scattering (DIS) has been measured by H1 in two ranges of the exchanged photon virtuality, $5 < Q^2 < 100\,\mathrm{GeV}^2$ [56] and $100 < Q^2 < 1000\,\mathrm{GeV}^2$ [57], using 2004-2007 data corresponding to an integrated luminosity of $350\,\mathrm{pb}^{-1}$. The data are described reasonably well by the NLO calculation HVQDIS [58].

The data description by the leading-order Monte-Carlo simulations RAPGAP and CASCADE [59] is satisfactory only in the low-Q^2 range. The measured $D^{*\pm}$ cross sections were used to extract the charm contribution to the proton structure, $F_2^{c\bar{c}}(x,Q^2)$, where x is the Bjorken scaling variable. The $F_2^{c\bar{c}}(x,Q^2)$ values in the frameworks of DGLAP and CCFM evolutions were obtained using for extrapolation HVQDIS and CASCADE, respectively.

H1 has also measured the inclusive charm cross sections simultaneously with the inclusive beauty cross sections in the range $5 < Q^2 < 650\,\mathrm{GeV}^2$ using the impact parameters and the secondary vertex position reconstructed with the H1 vertex detector [60]. To obtain fractions of charm, beauty and light quarks in the inclusive sample a neural network was used. The measured cross sections are described reasonably well by the predictions based on the DGLAP and CCFM evolutions. The charm and beauty contributions to the proton structure, $F_2^{c\bar{c}}(x,Q^2)$ and $F_2^{b\bar{b}}(x,Q^2)$, were extracted in the framework of DGLAP evolution. To gain in precision, the extracted $F_2^{c\bar{c}}(x,Q^2)$ values were combined with those obtained using the cross sections of $D^{*\pm}$ meson production [60]. The measurements were interpolated to the common x, Q^2 grid and averaged using the procedure developed for the inclusive F_2 taking into account correlations.

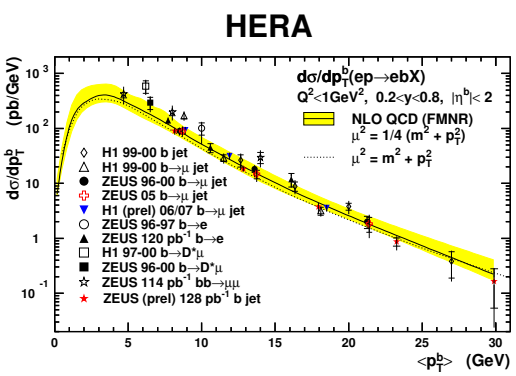

Figure 5: Summary of HERA differential cross sections for b-quark production in ep interactions in photoproduction regime as function of p_T^b as measured by H1 and ZEUS.

The production of $D^{\pm}$ and D^0 mesons in DIS has been measured by ZEUS in the range $5 < Q^2 < 1000\,\mathrm{GeV}^2$ using the ZEUS microvertex detector to reconstruct displaced secondary vertexes [61]. The measured cross sections were found to be in agreement with the predictions of NLO QCD with the proton parton density functions extracted from inclusive DIS data. The measured $D^{\pm}$ and D^0 cross sections were used to extract $F_2^{c\bar{c}}(x,Q^2)$ within the framework of DGLAP NLO QCD. The extracted $F_2^{c\bar{c}}(x,Q^2)$ values agree well with the previous measurements obtained using cross sections of $D^{*\pm}$ meson production.

ZEUS has also measured the production of charm and beauty quarks in DIS for $Q^2 > 20\,\mathrm{GeV}^2$ using the heavy-quark decays into muons [61, 62]. The fractions of muons originating from charm and beauty decays were determined using the muon momentum component transverse to the axis of the associated jet, the distance of closest approach of the muon track to the centre of the interaction region in the transverse plane and the missing transverse momentum parallel to the muon direction. The latter requirement was important for distinguishing contributions from charm and light flavours. The measured muon differential cross sections were compared to the NLO QCD calculations; the agreement was found to be good for charm and reasonable for beauty. The $F_2^{c\bar{c}}(x,Q^2)$ and $F_2^{b\bar{b}}(x,Q^2)$ values were also measured and found to agree well with other measurements based on independent techniques. The HERA measurements of $F_2^{c\bar{c}}$ and $F_2^{b\bar{b}}$ are summarised in Fig. 6.

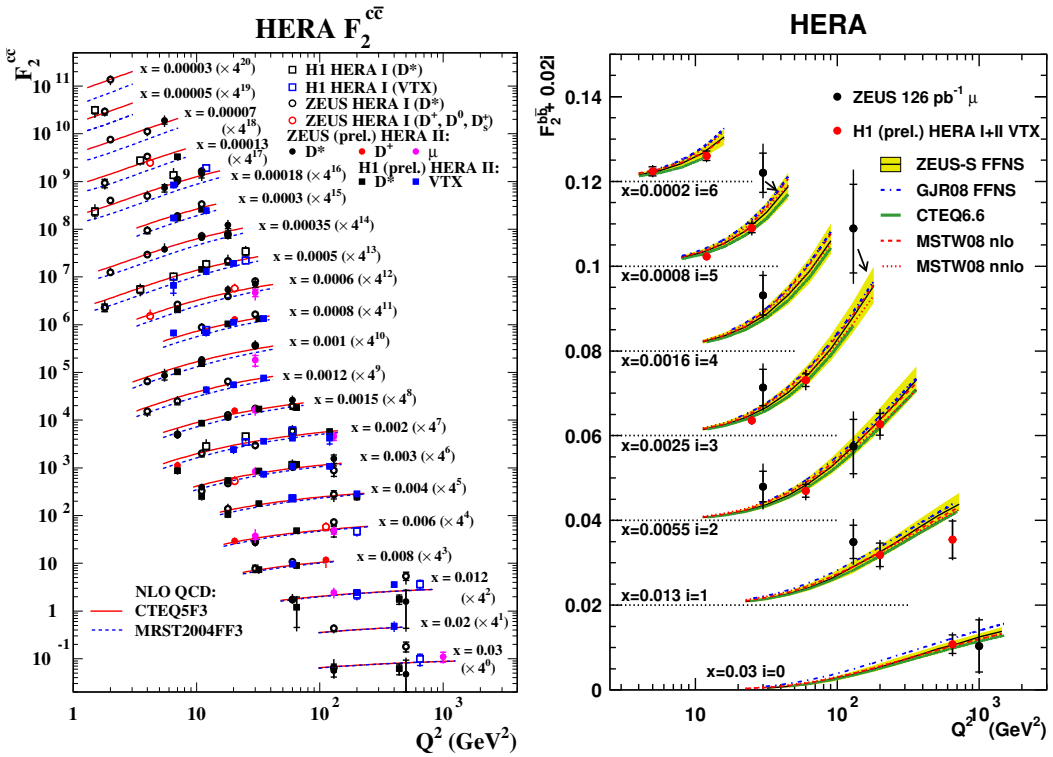

Figure 6: Summary of HERA measurements of the structure functions (left) $F_2^{c\bar{c}}$ and (right) $F_2^{b\bar{b}}$ plotted as functions of Q^2 for fixed x values.

Acknowledgements

We thank all speakers of the working group "Heavy flavours" for their talks and participation in discussions. Special thanks are due to the DIS 2009 organisers for their hospitality and help in running the sessions smoothly.

References

[1] Slides:
http://indico.cern.ch/contributionDisplay.py?contribId=19&sessionId=22&confId=53294
http://indico.cern.ch/contributionDisplay.py?contribId=331&sessionId=22&confId=53294
http://indico.cern.ch/contributionDisplay.py?contribId=332&sessionId=22&confId=53294

[2] B. A. Kniehl, G. Kramer, I. Schienbein and H. Spiesberger, Eur. Phys. J. C **41**, 199 (2005).

[3] H. Spiesberger, these proceedings.

[4] B. Kniehl, these proceedings.

[5] S. Alekhin, these proceedings.

[6] T. Toll, these proceedings.

[7] J. Pumplin, H. L. Lai and W. K. Tung, Phys. Rev. D **75**, 054029 (2007).

[8] W. K. Tung, H. L. Lai, A. Belyaev, J. Pumplin, D. Stump and C. P. Yuan, JHEP **0702**, 053 (2007).

[9] M. Buza, Y. Matiounine, J. Smith and W. L. van Neerven, Eur. Phys. J. C **1**, 301 (1998).

[10] P. Nadolsky, these proceedings.

[11] J. A. M. Vermaseren, A. Vogt and S. Moch, Nucl. Phys. B **724**, 3 (2005).

[12] S. Klein, these proceedings.

[13] I. Bierenbaum, J. Blumlein and S. Klein, [arXiv:0904.3563 [hep-ph]].

[14] T. Uematsu, these proceedings.

[15] E. Witten, Nucl. Phys. B **120** (1977) 189.

[16] Y. Kitadono, K. Sasaki, T. Ueda and T. Uematsu, Phys. Rev. D **77**, 054019 (2008).

[17] U. Langenfeld, these proceedings.

[18] U. Langenfeld, S. Moch and P. Uwer, [arXiv:0906.5273 [hep-ph]].

[19] A. D. Martin, W. J. Stirling, R. S. Thorne and G. Watt, [arXiv:0901.0002 [hep-ph]].

[20] P. M. Nadolsky *et al.*, Phys. Rev. D **78**, 013004 (2008).

[21] M. Krämer, Nucl. Phys. B **459**, 3 (1996).

[22] P. Artoisenet, J. M. Campbell, F. Maltoni and F. Tramontano, Phys. Rev. Lett. **102**, 142001 (2009).

[23] S. Chekanov *et al.* (ZEUS Collaboration), Eur. Phys. J. C **27**, 173 (2003).

[24] R. Brugnera (ZEUS collaboration), proceedings of XVIth. Int. Workshop on Deep-Inelastic-Scattering and Related Topics (DIS 2008), London, U.K.

[25] P. Artoisenet, these proceedings.

[26] J. Pumplin, D. R. Stump, J. Huston, H. L. Lai, P. M. Nadolsky and W. K. Tung, JHEP **0207**, 012 (2002).

[27] P. Faccioli, these proceedings.

[28] P. Faccioli, C. Lourenco, J. Seixas and H. K. Wohri, Phys. Rev. Lett. **102**, 151802 (2009).

[29] N. Zotov, these proceedings.

[30] M. Karliner *et al.* Ann. Phys. **394** 2 (2009);
M. Karliner, these proceedings.

[31] T. Aaltonen *et al.* (CDF Collaboration), [arXiv:0905.3123 [hep-ex]].

[32] V. M. Abazov *et al.* (D0 Collaboration), Phys. Rev. Lett. **101**, 232002 (2008).

[33] For a recent discussion of $X(3872)$ as a $D\bar{D}^*$ molecule, see, C. E. Thomas and F. E. Close, Phys. Rev. D **78**, 034007 (2008), and references quoted therein.

[34] L. Maiani, F. Piccinini, A. D. Polosa and V. Riquer, Phys. Rev. D **71**, 014028 (2005).

[35] A .D. Polosa, these proceedings.

[36] C. Bignamini, B. Grinstein, F. Piccinini, A. Polosa and C. Sabelli, [arXiv:0906.0882 [hep-ph]].

[37] T. Aaltonen *et al.* (CDF Collaboration), [arXiv:0903.0885 [hep-ex]];
V. M. Abazov *et al.* (D0 Collaboration), [arXiv:0903.0850 [hep-ex]];
G. Gómez and J. Kvita, these proceedings.

[38] V. M. Abazov *et al.* (D0 Collaboration), Phys. Rev. Lett. **101** 232002 (2008);
T. Aaltonen *et al.* (CDF Collaboration), Phys. Rev. Lett. **102** 242002 (2009);
P. Ratoff and K. Yi, these proceedings.

[39] J. P. Fernandez, J. He, C. Lourenço, M. Needham, T. Stahl, J. Andrea, and K. Toms, these proceedings.

[40] T. Aaltonen *et al.* (CDF Collaboration), Phys. Rev. Lett. **102** 242001 (2009);
J. Pinfold, these proceedings.

[41] A. Adare *et al.* (PHENIX Collaboration), [arXiv:0903.4851 [hep-ex]];
B. I. Abelev *et al.* (STAR Collaboration), [arXiv:0904.0439 [hep-ex]];
R. Granier de Cassagnac and J. Bielcik, these proceedings.

[42] M. Cacciari, P. Nason and R. Vogt, Phys. Rev. Lett. **95**, 122001 (2005).

[43] G. Bruno and C. Lourenço, these proceedings.

[44] J. Chen, these proceedings.

[45] T. Kuhr, these proceedings.

[46] E.S. Swanson, Phys. Lett. **B598** 197 (2004).

[47] V. Ziegler, these proceedings.

[48] R. Spighi, these proceedings.

[49] A. Bertolin, these proceedings.

[50] L. Gladilin, these proceedings.

[51] C. Peterson, D. Schlatter, I. Schmitt and P. M. Zerwas, Phys. Rev. D **27**, 105 (1983).

[52] P. Nason and C. Oleari, Nucl. Phys. **B565** 245 (2000).

[53] B. List, these proceedings.

[54] S. Miglioranzi, these proceedings.

[55] S. Frixione et al., Phys. Lett. **B348** 633 (1995);
S. Frixione, P. Nason and G. Ridolfi, Nucl. Phys. **B454** 3 (1995).

[56] A. Jung, these proceedings.

[57] M. Brinkmann, these proceedings.

[58] B. W. Harris and J. Smith, Nucl. Phys. **B452** 109 (1995).

[59] H. Jung and G. Salam, Eur. Phys. J. **C19** 351 (2001).

[60] P. D. Thompson, these proceedings.

[61] P. Roloff, these proceedings.

[62] M. Bindi, these proceedings.